



University of Dundee

Direct Monitoring of Protein O-GlcNAcylation by High-Resolution Native Mass Spectrometry

Leney, Aneika C.; Rafie, Karim; Van Aalten, Daan M.F.; Heck, Albert J. R.

Published in:
ACS Chemical Biology

DOI:
[10.1021/acscchembio.7b00371](https://doi.org/10.1021/acscchembio.7b00371)

Publication date:
2017

Document Version
Publisher's PDF, also known as Version of record

[Link to publication in Discovery Research Portal](#)

Citation for published version (APA):

Leney, A. C., Rafie, K., Van Aalten, D. M. F., & Heck, A. J. R. (2017). Direct Monitoring of Protein O-GlcNAcylation by High-Resolution Native Mass Spectrometry. *ACS Chemical Biology*, 12(8), 2078-2084. <https://doi.org/10.1021/acscchembio.7b00371>

General rights

Copyright and moral rights for the publications made accessible in Discovery Research Portal are retained by the authors and/or other copyright owners and it is a condition of accessing publications that users recognise and abide by the legal requirements associated with these rights.

- Users may download and print one copy of any publication from Discovery Research Portal for the purpose of private study or research.
- You may not further distribute the material or use it for any profit-making activity or commercial gain.
- You may freely distribute the URL identifying the publication in the public portal.

Take down policy

If you believe that this document breaches copyright please contact us providing details, and we will remove access to the work immediately and investigate your claim.

Direct Monitoring of Protein O-GlcNAcylation by High-Resolution Native Mass Spectrometry

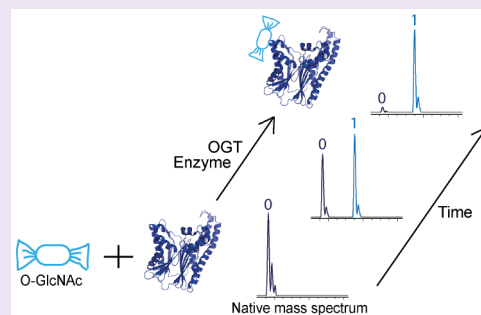
Aneika C. Leney,[†] Karim Rafie,[‡] Daan M. F. van Aalten,[‡] and Albert J. R. Heck^{*,†}

[†]Biomolecular Mass Spectrometry and Proteomics, Bijvoet Center for Biomolecular Research and Utrecht Institute for Pharmaceutical Sciences and Netherlands Proteomics Centre, Utrecht University, Padualaan 8, 3584 CH, Utrecht, The Netherlands

[‡]School of Life Sciences, University of Dundee, Dow Street, DD1 5EH, Dundee, United Kingdom

Supporting Information

ABSTRACT: O-GlcNAcylation is one of the most abundant metazoan nuclear-cytoplasmic post-translational modifications. Proteins modified by O-GlcNAc play key cellular roles in signaling, transcription, metabolism, and cell division. Mechanistic studies on protein O-GlcNAcylation are hampered by the lack of methods that can simultaneously quantify O-GlcNAcylation, determine its stoichiometry, and monitor O-GlcNAcylation kinetics. Here, we demonstrate that high-resolution native mass spectrometry can be employed to monitor the small mass shifts induced by modification by O-GlcNAc on two known protein substrates, CK2 α and TAB1, without the need for radioactive labeling or chemoenzymatic tagging using large mass tags. Limited proteolysis enabled further localization of the O-GlcNAc sites. In peptide-centric MS analysis, the O-GlcNAc moiety is known to be easily lost. In contrast, we demonstrate that the O-GlcNAc is retained under native MS conditions, enabling precise quantitative analysis of stoichiometry and O-GlcNAcylation kinetics. Together, the data highlight that high resolution native MS may provide an alternative tool to monitor kinetics on one of the most labile of protein post-translational modifications, in an efficient, reliable, and quantitative manner.



Post-translational modifications are vital cell communication signals that can transfer messages between proteins enabling signaling pathways to be turned on or off. Protein O-GlcNAcylation is a dynamic modification, whereby N-acetyl-D-glucosamine cycles on and off serine or threonine residues on proteins and is of prominent interest due to its role in diabetes, cardiovascular disease, neurodegenerative diseases, and cancer.^{1–3} Two enzymes act synergistically to regulate protein O-GlcNAcylation in cells; the O-GlcNAc transferase (OGT) installs an O-GlcNAc moiety onto proteins using UDP-GlcNAc as a donor substrate, and a glycoside hydrolase termed O-GlcNAcase catalyzes O-GlcNAc removal.^{4,5}

Despite its discovery over 30 years ago, relatively few novel O-GlcNAcylated proteins were identified immediately thereafter. This was primarily due to the lack of sensitive and quantitative methods for monitoring protein O-GlcNAcylation. Initial biochemical methods to monitor O-GlcNAcylation involved enzymatic tagging of the protein O-GlcNAc site with radiolabeled galactose.⁶ The pure radiolabeled protein was then subjected to proteolysis, the peptides purified, and these peptides sequenced by Edman degradation.⁷ This method, albeit successful at identifying O-GlcNAcylated proteins, is very time-consuming and thus of low-throughput. More recently, O-GlcNAc antibodies have been introduced, which have aided rapid visualization of protein O-GlcNAcylation using Western blotting.^{8,9} However, stoichiometric determination and precise O-GlcNAc quantitation by Western blotting is not trivial, given

that the binding affinity of antibodies to O-GlcNAc is low, preventing the use of stringent washing procedures that are required for the reduction of nonspecific interactions. In addition, due to the limited availability of site-specific O-GlcNAc antibodies,¹⁰ mapping the sites of O-GlcNAcylation of proteins by these methods and determining stoichiometry is notoriously difficult.

Over the past decade, peptide-centric mass spectrometry has been used extensively for the detection and site-mapping of post-translational modifications.^{11–14} In these peptide-centric approaches, all proteins present are first digested into peptides, often followed by an enrichment step for the modified peptides, and subsequently analyzed by LC MS/MS. Especially for protein phosphorylation, such methods have proven to be very powerful.¹⁵ However, these methodologies were initially not easily transferable for the detection of O-GlcNAc moieties, due to the very facile loss of the O-GlcNAc during CID/HCD fragmentation. To circumvent this, methods have been developed whereby the O-GlcNAc moiety is deliberately released by β -elimination and the site then marked by Michael Addition (BEMAD).^{16,17} These modified peptides can then be enriched and the sites mapped using LC-MS/MS. This breakthrough enabled numerous O-GlcNAcylated proteins to

Received: May 5, 2017

Accepted: June 13, 2017

Published: June 13, 2017

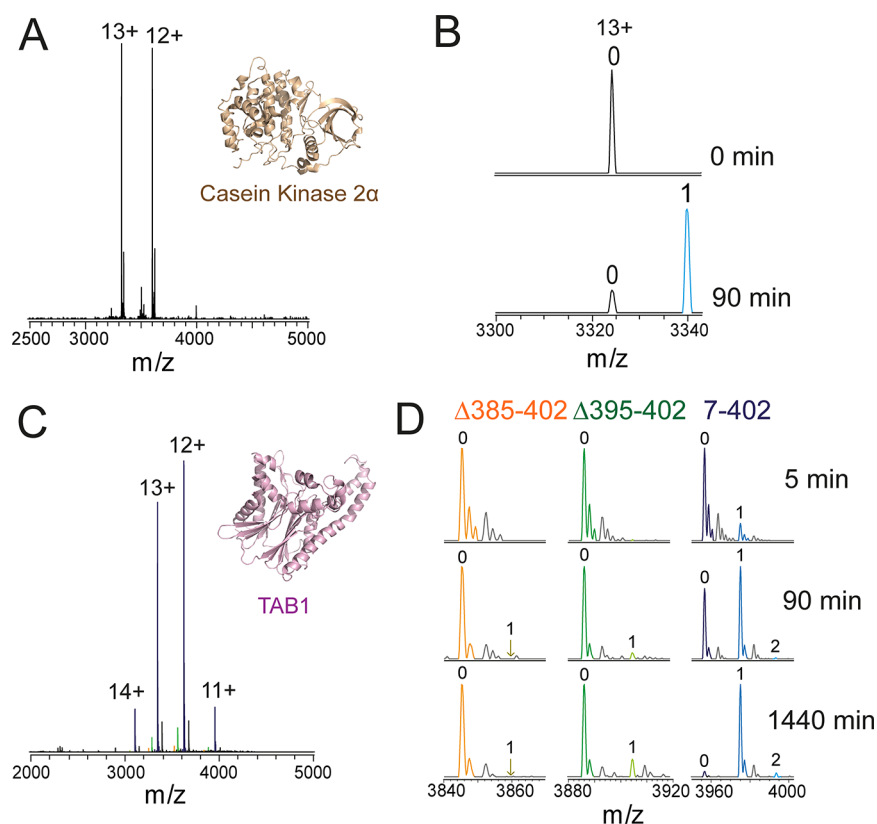


Figure 1. Temporal profiling of protein O-GlcNAcylation by native MS. Native ESI-MS spectra of CK2 α (A) and upon incubation with the O-GlcNAc transferase after 0 and 90 min (B). Native ESI-MS spectra of TAB1 (C) and upon incubation with the O-GlcNAc transferase after 5, 90, and 1440 min (D). Peaks corresponding to the unmodified and the emerging peaks of one and two O-GlcNAc moieties on the intact proteins upon incubation are labeled 0, 1, and 2, respectively. Peaks corresponding to C-terminal degradation of TAB1 are highlighted for TAB1 Δ 395–402 and Δ 385–402 in green and orange, respectively.

be identified even in mitochondria.¹⁸ However, care needs to be taken since O-GalNAc and O-phosphate can also be released by β -elimination, making the BEMAD method prone to the identification of false positive O-GlcNAcylation sites. Thus, the direct monitoring of O-GlcNAcylation sites on proteins is still preferential. This has been made possible at the peptide level through advancements in MS/MS fragmentation techniques, notably the introduction of ECD/ETD fragmentation.^{19,20} Combined with metabolic labeling, carbohydrate-based enrichment methods,²¹ or chemoenzymatic tagging of O-GlcNAc-based enrichment strategies,²² over 200 O-GlcNAcylation sites can now be identified in a single experiment.²³ Although rich in information in terms of the number of O-GlcNAcylated proteins that can be monitored, these peptide-centric LC MS/MS studies lack information on the overall O-GlcNAc stoichiometry. Moreover, even when different O-GlcNAcylated peptides reveal that multiple sites can be occupied on a single protein, it remains unresolved whether these are present simultaneously on the intact protein. Recent advancements in chemoenzymatic labeling whereby relatively large mass tags (2–5 kDa) are conjugated to the O-GlcNAc moiety on proteins has enabled the determination of the O-GlcNAc stoichiometry on intact proteins.²⁴ In this work, mono-, di-, tri-, and tetraglycosylated forms of the purified cAMP-response element binding protein (CREB) were resolved by SDS-PAGE and their relative abundances determined by Western blotting using an anti-CREB antibody. This quantitative analysis by enzymatic labeling has some caveats as it is based on the assumption that the chemo-enzymatic labeling of the O-

GlcNAc moiety is 100% complete and that the addition of a 2–5 kDa mass tag does not interfere with antibody binding during Western blotting.

Native MS, a technique in which proteins and protein complexes are mass analyzed directly from a nondenaturing solution,²⁵ offers the potential to monitor O-GlcNAcylation at the intact protein level, providing information at both the structural and kinetic level. Monitoring O-GlcNAcylation by native MS requires first of all good mass accuracy. In addition, since the mass shift (+203 Da) characteristic of O-GlcNAcylation is relatively small compared with large proteins and protein complexes, high mass resolving power is needed, to differentiate and quantify different co-occurring O-GlcNAcylated proteoforms. Recent instrumental advances in Orbitrap mass analyzers with an extended mass range have enabled for large proteins and protein complexes higher mass resolving power to be achieved compared with conventional Q-ToF instrumentation.²⁶ This has proven advantageous when monitoring post-translational modifications, for instance N-glycosylation on antibodies²⁷ and phosphorylation on kinases and noncovalent protein complexes.²⁸ Here, we show that with high-resolution native mass spectrometry, baseline resolution of differential O-GlcNAcylated proteoforms can be achieved on intact proteins. To demonstrate the potential of our method, we chose two well-known protein substrates of the O-GlcNAc transferase enzyme: TAB1 and CK2 α .^{29,30} TAB1 binds to the transforming growth factor (TGF)- β -activated kinase 1, TAK1, a key regulator of inflammatory and immunity signaling pathways.³¹ Indeed, O-GlcNAcylation at Ser395 on TAB1 has

been shown to increase TAK1 activation, enhancing cytokine release.²⁹ Casein kinase II (CK2) is a ubiquitously expressed kinase that phosphorylates hundreds to thousands of protein substrates.³² CK2 is a tetramer comprising two CK2 α and two CK2 β subunits whereby CK2 α , the catalytic subunit, is active in both its monomeric form and when bound to CK2 β .³³ It has been hypothesized that O-GlcNAcylation of CK2 α at Ser347, adjacent to particular phosphorylation sites on CK2 α , may play a role in regulating CK2 activity.³⁰ Together, we show the advantages of native MS in monitoring O-GlcNAcylation, highlighting its ability to determine O-GlcNAcylation stoichiometry on proteins while simultaneously being able to quantify O-GlcNAcylation kinetics.

RESULTS AND DISCUSSION

Native MS Reveals O-GlcNAcylation Stoichiometry.

We overexpressed and purified CK2 α from *E. coli*, leading to a very clean native MS spectrum displaying a narrow charge state distribution (12+ and 13+ charge state ions) corresponding to a molecular weight of 43202.3 Da, which is within 0.002% of the calculated mass based on the sequence (43203.2 Da; Figure 1A, Supporting Information Figure 1). Next, to monitor O-GlcNAcylation, CK2 α was incubated with O-GlcNAc transferase in the presence of UDP-GlcNAc for 90 min. The resulting O-GlcNAcylated CK2 α protein (Figure 1B) could be clearly mass-separated from the free CK2 α and revealed that O-GlcNAcylation of CK2 α occurs readily, resulting in a 1:1 stoichiometry. Although this hints at the presence of just one kinetically favorable O-GlcNAcylation site on CK2 α , this single modification could theoretically be distributed over multiple O-GlcNAcylation acceptor sites. Thus, complementary tryptic digestion of CK2 α followed by LC-MS/MS analysis of the resulting peptides was carried out to localize the exact sites of O-GlcNAcylation on CK2 α . A single O-GlcNAc site on the C-terminal region of CK2 α (residues 334–365; Supporting Information Figure 2) was observed, consistent with previous studies confining O-GlcNAcylation to Ser347.³⁰ The observation of only a single O-GlcNAcylation site on CK2 α is striking considering that CK2 α contains 38 Ser/Thr residues, all of which could potentially be O-GlcNAcylated. To determine whether the CK2 α tertiary structure alone prevents O-GlcNAcylation of Ser/Thr residues, we next digested the CK2 α protein into a series of peptides through digestion with LysC. The resulting mixtures of peptides were incubated with the O-GlcNAc transferase in the presence of UDP-GlcNAc. Crucially, out of all 50 detected peptides originating from the CK2 α digest, only one (covering residues 334–365) was found to become O-GlcNAcylated (Supporting Information Figure 3). Thus, consistent with recent findings using peptide libraries,³⁴ O-GlcNAc transferase must impart not only structural but also quite specific sequence constraints on its substrates. To put this finding in a context, we note that in *in vitro* kinase assays, more promiscuity is often observed, whereby next to some preferred sites, many more Ser/Thr become phosphorylated.³⁵

Also, TAB1 (residues 7–402) was expressed and highly purified. The resulting native mass spectrum of TAB1 again shows a narrow charge state distribution (11+ to 14+ charge state ions) corresponding to a molecular weight of 43510.2 Da, which is within 0.004% of the calculated mass based on the sequence (43511.9 Da; Figure 1C). In these spectra, small satellite peaks were also observed corresponding to TAB1 residues 7–384 (orange) and residues 7–394 (green), hereafter

referred to as TAB1 Δ 385–402 and TAB1 Δ 395–402, respectively. These peaks were attributed to C-terminal degradation during the recombinant TAB1 expression and purification process. Upon incubation of TAB1 with O-GlcNAc transferase, mass shifts appeared with time corresponding to TAB17–402 with a single O-GlcNAc site (blue; Figure 1D, Supporting Information Figure 4). Minor peaks were also observed corresponding to the addition of two O-GlcNAc sites on TAB17–402 (pale blue). The peaks corresponding to doubly O-GlcNAcylated TAB17–402 correspond to less than 5% of the overall signal intensity, indicating the gross O-GlcNAcylation stoichiometry for TAB1 is 1:1. Interestingly, the C-terminal truncated protein TAB1 Δ 385–402 did not undergo O-GlcNAcylation at all, in contrast to TAB1 Δ 395–402, where only one O-GlcNAc moiety became attached (Figure 1D). Thus, from the native mass spectra, we concluded that both O-GlcNAcylation sites are at the C-terminal 385–402 residues of TAB1: one site between residues 385 and 394 (i.e., Ser391) and the other site on residues 395–402.

Limited Proteolysis Enables Rapid Localization of O-GlcNAc Sites. Since O-GlcNAcylation typically occurs on unstructured regions of proteins,³⁶ we hypothesized that limited proteolysis in combination with native MS could be a fruitful tool for rapid identification of O-GlcNAcylation regions on proteins. Limited proteolysis is widely used to identify flexible, intrinsically disordered regions of proteins.³⁷ To determine the specific regions/domains on TAB1 and CK2 α where O-GlcNAcylation occurs, limited trypsin proteolysis was performed whereby TAB1 and CK2 α were incubated for 15 min on ice in a 1:200 trypsin/protein ratio, and the resulting precursor and cleaved TAB1/CK2 α products were analyzed by native MS (Supporting Information Figure 5). For both TAB1 and CK2 α , the first cleavage site corresponding presumably to the most flexible, intrinsically disordered region of the protein was identified to be on the C-terminus. Indeed, this is in support of crystallographic studies whereby the C-terminal residues of CK2 α and TAB1 could not be structurally resolved, possibly due to conformational diversity.^{38,39} To show the applicability of limited proteolysis for rapid identification of the O-GlcNAcylation regions on proteins, limited proteolysis was performed on a 50/50 mixture of unmodified and O-GlcNAc modified TAB1 and the cleavage products analyzed by high resolution MS (Figure 2A). Upon analysis of the intact proteins, two peaks were clearly visible in a 50:50 ratio corresponding to the full length (black) and singly O-GlcNAcylated (blue) TAB17–402 protein. In contrast, only one peak was observed for the C-terminally cleaved TAB1 Δ 387–402 protein (purple) showing that the O-GlcNAc moiety is located on the C-terminal 15 residues of TAB17–402. Consistent with this, two major peaks were observed at low *m/z* in a 1:1 ratio corresponding to the free (purple) and O-GlcNAcylated (blue) C-terminal TAB1 peptide (residues 387–402). Thus, from a single limited proteolysis mass spectrum, we can not only measure O-GlcNAcylation stoichiometry but also rapidly locate the O-GlcNAcylation site on TAB1 to the unstructured C-terminus.

Labile O-GlcNAc Moiety Maintained at Protein Level.

To extract quantitative information on O-GlcNAcylation kinetics from native MS data, it is imperative that the O-GlcNAc moiety is not eliminated prior to mass analysis. This is not trivial, as it has been shown that with MS/MS fragmentation methods such as CID and HCD, the O-GlcNAc moiety, due to its labile nature, is readily lost from peptides.⁴⁰

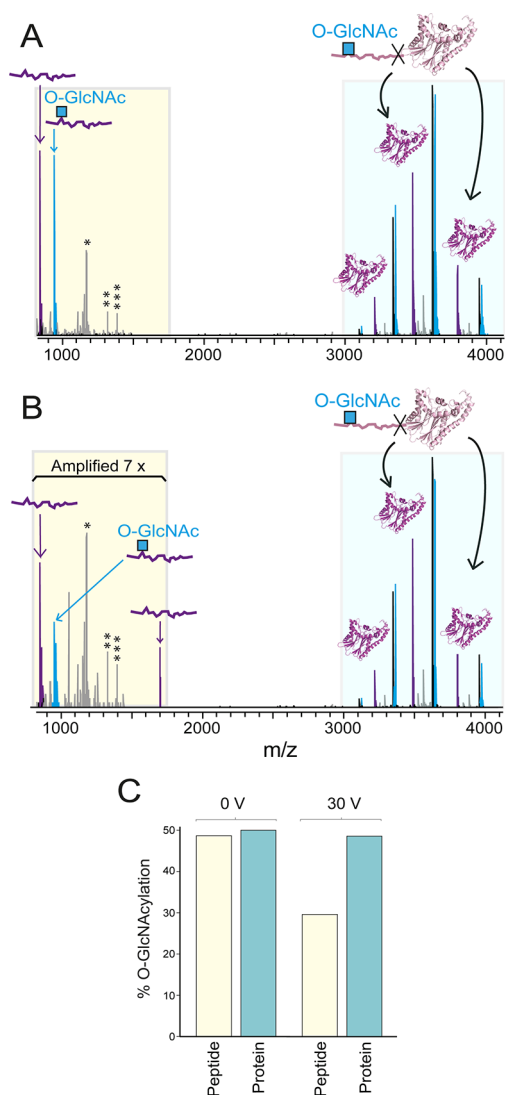


Figure 2. Simultaneous profiling of protein O-GlcNAcylation at the protein and peptide level revealing instability of the modification at the peptide level. Native MS spectra of TAB1, following limited proteolysis of TAB1, after 50 min incubation with the O-GlcNAc transferase. Mass spectra were acquired at a HCD voltage of 0 V (A) and 30 V (B). The ions corresponding to peptides and proteins are clearly separated in m/z ; highlighted by a yellow/blue box background. Peaks corresponding to the main TAB1 trypsin cleavage products are shown in purple. Blue peaks correspond to the O-GlcNAc modified peptide (res387–402) and the TAB1 protein (res7–402). *, **, and *** represent the minor peptide cleavage products: res1–33, Δ 365–402, and O-GlcNAc- Δ 365–402, respectively. (C) Percentage of O-GlcNAc modified TAB1 detected on the intact protein and peptide level at 0 and 30 V, revealing the specific loss of the O-GlcNAc moiety at the peptide level.

Moreover, on shorter O-GlcNAcylated peptides, the O-GlcNAc moiety can be lost even prior to precursor ion selection. To exemplify this, the percentage of O-GlcNAcylation on TAB1 was compared between native MS and LC-MS measurements whereby O-GlcNAcylated TAB1 had been digested into peptides using trypsin (Supporting Information Figure 6). Less than 1% O-GlcNAcylation was observed on the tryptic peptide TAB1 res387–394 compared with the 20% O-GlcNAcylation that was detected by native MS on the intact TAB1 Δ 395–402 protein.

To investigate further the potential instability of the O-GlcNAc moiety during native MS analysis, the stoichiometry of O-GlcNAcylated TAB1 protein was measured as a function of HCD energy (Figure 2B, C). Interestingly, the ratio of O-GlcNAcylated versus unmodified TAB1 protein remained constant upon increasing the collision energy from 0 V (Figure 2A) to 175 V (Figure 2B and Supporting Information Figure 7). This is striking as already at 30 V collision energy over 40% of the O-GlcNAc moieties were released from the corresponding O-GlcNAcylated C-terminal peptide (Figure 2 and Figure S7). These differences in the gas phase stabilities of the O-GlcNAcylated proteins and peptides can be largely attributed to the relative energy distribution across the peptide/protein backbone during slow heating MS/MS methods such as HCD.⁴¹ Generally speaking, if the same energy is applied, the O-GlcNAc moiety on a small peptide will attain more internal energy (and thus will be more prone to dissociation) than an O-GlcNAc moiety on a protein. As such, native MS can monitor quantitatively O-GlcNAcylation, a modification that has been proven to be highly challenging to monitor quantitatively at the peptide level.⁴⁰

O-GlcNAcylation Kinetics Monitored by Native MS. To further illustrate the ability of native MS in quantitatively monitoring O-GlcNAcylation kinetics, the percentage O-GlcNAcylation of TAB17–402 (blue), TAB1 Δ 385–402 (orange), and TAB1 Δ 395–402 (green) incubated in a single vial with the O-GlcNAc transferase was determined and plotted as a function of the reaction time (Figure 3A). Interestingly, the rate of O-GlcNAcylation of these three constructs differed: no O-GlcNAcylation was detected at all on TAB1 Δ 385–402; 20% of TAB1 Δ 395–402 was O-GlcNAcylated only after 24 h of incubation with O-GlcNAc transferase, and the O-GlcNAcylation reaction with TAB17–402 reached completion within 8 h of incubation with O-GlcNAc transferase. As previously stated, due to the difference in primary sequence between TAB1 Δ 385–402 and TAB1 Δ 395–402, O-GlcNAcylation on TAB1 Δ 395–402 can be mapped to Ser391. Since two O-GlcNAcylation sites were observed on TAB17–402 (Figure 1D), we attributed one site to Ser391 and the other to one of the four Ser/Thr residues located between residues 395–402 on TAB1. Upon trypsin digestion of TAB1 followed by LC-MS/MS in combination with ETD, the second O-GlcNAcylation site on TAB1 could be mapped to residue Ser395 (Supporting Information Figure 8). Furthermore, this is consistent with our previous work,²⁹ whereby a single O-GlcNAcylation site on TAB1 was mapped to Ser395. Interestingly, lower abundant fragment ions were also observed corresponding to Ser391 O-GlcNAcylation (Supporting Information Figure 8), supporting our argument that the two O-GlcNAcylation sites observed by native MS on TAB1 are located on Ser391 and Ser395. Since the O-GlcNAcylation reaction of TAB17–402 (i.e., Ser391 and Ser395 O-GlcNAcylation) reaches completion on a shorter time scale than TAB1 Δ 395–402 (i.e., Ser391 O-GlcNAcylation), we consider Ser395 and Ser391 to be the primary (fast kinetics) and secondary (slower kinetics) O-GlcNAcylation sites, respectively.

An alternative, albeit less direct, method to monitor the kinetics of O-GlcNAcylation for TAB1 would be to digest the O-GlcNAcylated protein of interest at various time points during the O-GlcNAcylation reaction and analyze the extent of O-GlcNAcylation at the peptide level using LC-MS. Thus, for comparison, the O-GlcNAcylated TAB1 native MS samples at

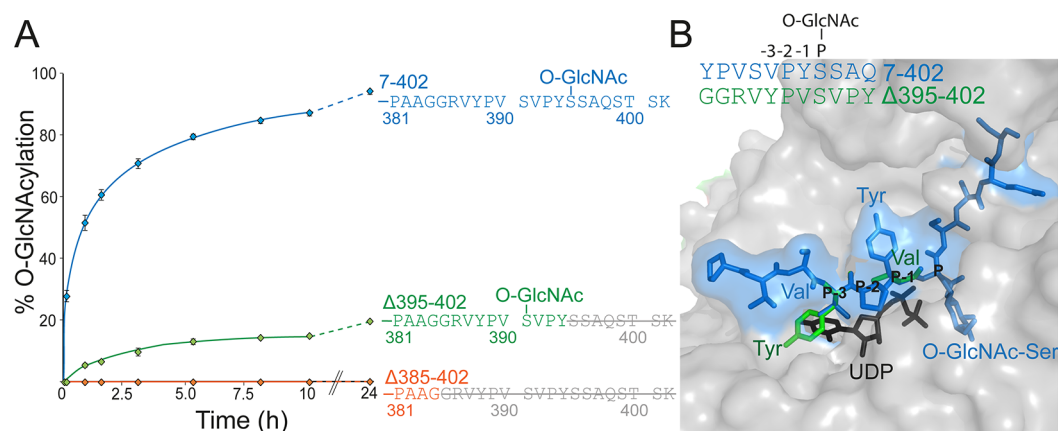


Figure 3. Sequence context has a profound effect on the kinetics of O-GlcNAcylation. (A) O-GlcNAcylation kinetics of TAB1 for res7–402 (blue) and the C-terminally truncated TAB1 proteins Δ 395–402 (green) and Δ 385–402 (orange). (B) O-GlcNAc transferase active site (gray) showing the glycopeptide from TAB1 bound (blue) on top of UDP (black) (PDB 4AYS). The positions of the amino acids relative to the Ser395 O-GlcNAcylation site are labeled P, P-1, P-2, and P-3. The P-1 and P-3 positions were substituted from Tyr and Val to Val (at P-1) and Tyr (at P-3), respectively, (green) to mimic the situation whereby Ser391 is O-GlcNAcyated.

various time points were digested with trypsin and analyzed by LC-MS. Two TAB1 peptides were observed corresponding to the O-GlcNAcyated TAB1 peptides res387–402 and res387–394 (Supporting Information Figure 6A, C). Upon plotting the % O-GlcNAcylation of the TAB1 peptide res387–402 over time, very similar kinetics were observed compared with those when measured on the intact TAB17–402 protein by native MS (Figure 3, Supporting Information Figure 6B). In sharp contrast to the native MS on TAB1 Δ 395–402 whereby 15% O-GlcNAcylation was observed after 10 h, no O-GlcNAcylation was observed on the TAB1 peptide res387–394 at the same time point. This difference is attributed to the difference in stability of the O-GlcNAc moiety in the gas phase at the protein/peptide level (Figure 2). Thus, native MS is advantageous over traditional peptide-centric approaches in not only quantifying O-GlcNAcylation but also in monitoring O-GlcNAcylation kinetics.

The difference in O-GlcNAcylation kinetics between residues Ser395 and Ser391 (Figure 3A) is somewhat surprising considering the high sequence similarity: –Y–P–V–S– versus –V–P–Y–S– for the O-GlcNAc sites at Ser391 and Ser395, respectively (Table S1). Since Pro is conserved at the P-2 position, we attribute the differing rates of O-GlcNAcylation to the differences at the P-3 and P-1 positions. Overlaying the valine at the P-3 position (when Ser395 O-GlcNAcyated) with tyrosine (residue present when Ser391 O-GlcNAcyated) in the crystal structure of the TAB1 glycopeptide bound in the active site of O-GlcNAc transferase (Figure 3B) shows the steric clashes that would occur with UDP when a bulky side chain such as that on tyrosine is introduced in this position. Thus, the nature of the amino acid at the P-3 is imperative for fast O-GlcNAcylation kinetics. It is possible that the truncation of the C-terminal residues of TAB1 prevent the interactions needed for Ser391 to fit into the O-GlcNAc transferase active site. However, evidence suggests this is not the case considering the O-GlcNAc residue predominantly resides on Ser395 in the TAB17–402 protein (Supporting Information Figure 8), and the signal contributing to the O-GlcNAcyated protein with two O-GlcNAcylation sites is less than 5% of the total signal intensity after 24 h (Supporting Information Figure 4).

Conclusions. In summary, we demonstrate that high resolution native MS is a promising addition to the toolbox

for monitoring O-GlcNAcylation of protein substrates uniquely providing information on O-GlcNAc stoichiometry and O-GlcNAcylation kinetics. In comparison with established QToF instrumentation (Supporting Information Figure 9), baseline resolution was obtained using the Orbitrap EMR mass analyzer enabling O-GlcNAc proteoforms to be identified and quantified on larger intact proteins. Although, the *in vitro* approach requires protein (over)expression and proteins of high purity, with current instrumentation, the obtained mass resolving power would enable analysis of O-GlcNAc proteoforms on proteins and protein complexes of up to 200 kDa to be measurable using the Orbitrap EMR.

Beneficially, native MS preserves the labile O-GlcNAc on proteins allowing it to be quantified precisely. Finally, since no label has been incorporated that specifically targets O-GlcNAcylation, we believe that the methodology presented here is widely applicable to monitoring multiple post-translational modifications that may occur independently or simultaneously to O-GlcNAcylation on proteins and protein complexes, thus enabling investigations into cross-talk between different post translational modifications.⁴²

EXPERIMENTAL DETAILS

TAB1, CK2, and OGT were purified as described previously.^{29,30,34} *In vitro* O-GlcNAcylation assays were performed at 37 °C at physiological pH in the presence of 50-fold molar excess of UDP-GlcNAc using a 1:1 and 1:5 enzyme/substrate ratio for the reactions with TAB1 and CK2 α , respectively. Reactions were quenched on ice and rapidly buffer exchanged into ammonium acetate at pH 8.0 for analysis on an Orbitrap EMR mass spectrometer. To create the library of peptides from CK2 α for the peptide O-GlcNAcylation reactions, CK2 α (in 100 mM ammonium acetate at pH 8.0) was digested with LysC overnight in a 1:50 LysC/CK2 α ratio. LysC was then deactivated through heating to 95 °C for 5 min, the solution cooled, and the O-GlcNAcylation reaction then carried out as previously described. The peptides were analyzed by direct infusion using a nanoESI source coupled to an Orbitrap EMR mass spectrometer.

For limited proteolysis experiments, the O-GlcNAcylation reaction was quenched when the ratio of free/O-GlcNAcyated proteins reached 1:1 (i.e., 50 min after addition of O-GlcNAc transferase for TAB1). Trypsin was then added in a 1:200 trypsin/protein ratio. After 15 min of incubation on ice, native mass spectra were immediately acquired. To monitor the relative stability of the O-GlcNAcyated peptides and proteins, the MS settings were optimized for efficient

transmission of low and high m/z ions, and the HCD voltage increased systematically from 0 to 175 V without precursor ion selection. For identification of the O-GlcNAcylation sites, TAB1 and CK2 α were digested with trypsin and the reaction quenched by the addition of 10% formic acid prior to LC-MS/MS analysis. The samples were analyzed on a LTQ-Orbitrap Elite coupled to an EASY-nLC 1000. More detailed experimental details are available in the [Supporting Information](#).

■ ASSOCIATED CONTENT

■ Supporting Information

The Supporting Information is available free of charge on the ACS Publications website at DOI: [10.1021/acschembio.7b00371](https://doi.org/10.1021/acschembio.7b00371).

Experimental details and annotated spectra ([PDF](#))

■ AUTHOR INFORMATION

■ Corresponding Author

*E-mail: a.j.r.heck@uu.nl.

■ ORCID

Albert J. R. Heck: [0000-0002-2405-4404](https://orcid.org/0000-0002-2405-4404)

■ Notes

The authors declare no competing financial interest.

■ ACKNOWLEDGMENTS

We kindly thank M. Schimpl for expressing and purifying the protein CK2 α used in this study. D.v.A. is supported by a Wellcome Trust Investigator Award (110061). This work was supported by the Roadmap Initiative Proteins@Work (project number 184.032.201), funded by The Netherlands Organization for Scientific Research (NWO). Additionally, we acknowledge support from the MSMed program, funded by the European Union's Horizon 2020 Framework Programme (grant agreement number 686547).

■ REFERENCES

- (1) Slawson, C., Copeland, R. J., and Hart, G. W. (2010) O-GlcNAc signaling: a metabolic link between diabetes and cancer? *Trends Biochem. Sci.* *35*, 547–555.
- (2) Dassanayaka, S., and Jones, S. P. (2014) O-GlcNAc and the cardiovascular system. *Pharmacol. Ther.* *142*, 62–71.
- (3) Yuzwa, S. A., and Vocadlo, D. J. (2014) O-GlcNAc and neurodegeneration: biochemical mechanisms and potential roles in Alzheimer's disease and beyond. *Chem. Soc. Rev.* *43*, 6839–6858.
- (4) Lazarus, M. B., Nam, Y., Jiang, J., Sliz, P., and Walker, S. (2011) Structure of human O-GlcNAc transferase and its complex with a peptide substrate. *Nature* *469*, 564–567.
- (5) Alonso, J., Schimpl, M., and van Aalten, D. M. F. (2014) O-GlcNAcase: promiscuous hexosaminidase or key regulator of O-GlcNAc signaling? *J. Biol. Chem.* *289*, 34433–34439.
- (6) Torres, C. R., and Hart, G. W. (1984) Topography and polypeptide distribution of terminal N-acetylglucosamine residues on the surfaces of intact lymphocytes. Evidence for O-linked GlcNAc. *J. Biol. Chem.* *259*, 3308–3317.
- (7) Sullivan, S., and Wong, T. W. (1991) A manual sequencing method for identification of phosphorylated amino acids in phosphopeptides. *Anal. Biochem.* *197*, 65–68.
- (8) Snow, C. M., Senior, A., and Gerace, L. (1987) Monoclonal antibodies identify a group of nuclear pore complex glyco-proteins. *J. Cell Biol.* *104*, 1143–1156.
- (9) Comer, F. I., Vosseller, K., Wells, L., Accavitti, M. A., and Hart, G. W. (2001) Characterization of a mouse monoclonal antibody specific for O-linked N-acetylglucosamine. *Anal. Biochem.* *293*, 169–177.
- (10) Teo, C. F., Ingale, S., Wolfert, M. A., Elsayed, G. A., Nöt, L. G., Chatham, J. C., Wells, L., and Boons, G.-J. (2010) Gly-copeptide-

specific monoclonal antibodies suggest new roles for O-GlcNAc. *Nat. Chem. Biol.* *6*, 338–343.

(11) Witze, E. S., Old, W. M., Resing, K. A., and Ahn, N. G. (2007) Mapping protein post-translational modifications with mass spectrometry. *Nat. Methods* *4*, 798–806.

(12) Olsen, J. V., and Mann, M. (2013) Status of large-scale analysis of post-translational modifications by mass spectrometry. *Mol. Cell. Proteomics* *12*, 3444–3452.

(13) Zhang, Y., Fonslow, B. R., Shan, B., Baek, M.-C., and Yates, J. R. (2013) Protein analysis by shotgun/bottom-up proteomics. *Chem. Rev.* *113*, 2343–2394.

(14) Doll, S., and Burlingame, A. L. (2015) Mass spectrometry-based detection and assignment of protein posttranslational modifications. *ACS Chem. Biol.* *10*, 63–71.

(15) Grimsrud, P. A., Swaney, D. L., Wenger, C. D., Beauchene, N. A., and Coon, J. J. (2010) Phosphoproteomics for the masses. *ACS Chem. Biol.* *5*, 105–119.

(16) Wells, L., Vosseller, K., Cole, R. N., Cronshaw, J. M., Matunis, M. J., and Hart, G. W. (2002) Mapping sites of O-GlcNAc modification using affinity tags for serine and threonine post-translational modifications. *Mol. Cell. Proteomics* *1*, 791–804.

(17) Greis, K. D., Hayes, B. K., Comer, F. I., Kirk, M., Barnes, S., Lowary, T. L., and Hart, G. W. (1996) Selective detection and site-analysis of O-GlcNAc-modified glycopeptides by beta-elimination and tandem electrospray mass spectrometry. *Anal. Biochem.* *234*, 38–49.

(18) Cao, W., Cao, J., Huang, J., Yao, J., Yan, G., Xu, H., and Yang, P. (2013) Discovery and Confirmation of O-GlcNAcylated Proteins in Rat Liver Mitochondria by Combination of Mass Spectrometry and Immunological Methods. *PLoS One* *8*, e76399.

(19) Chalkley, R. J., Thalhammer, A., Schoepfer, R., and Burlingame, A. L. (2009) Identification of protein O-GlcNAcylation sites using electron transfer dissociation mass spectrometry on native peptides. *Proc. Natl. Acad. Sci. U. S. A.* *106*, 8894–8899.

(20) Ma, J., and Hart, G. W. (2017) Analysis of Protein O-GlcNAcylation by Mass Spectrometry. *Curr. Protoc. Protein Sci.* *87*, 24.10.1–24.10.16.

(21) Vocadlo, D. J., Hang, H. C., Kim, E.-J., Hanover, J. A., and Bertozzi, C. R. (2003) A chemical approach for identifying O-GlcNAc-modified proteins in cells. *Proc. Natl. Acad. Sci. U. S. A.* *100*, 9116–9121.

(22) Tai, H.-C., Khidekel, N., Ficarro, S. B., Peters, E. C., and Hsieh-Wilson, L. C. (2004) Parallel identification of O-GlcNAc-modified proteins from cell lysates. *J. Am. Chem. Soc.* *126*, 10500–10501.

(23) Hahne, H., Sobotzki, N., Nyberg, T., Helm, D., Borodkin, V. S., van Aalten, D. M. F., Agnew, B., and Kuster, B. (2013) Proteome wide purification and identification of O-GlcNAc-modified proteins using click chemistry and mass spectrometry. *J. Proteome Res.* *12*, 927–936.

(24) Rexach, J. E., Rogers, C. J., Yu, S.-H., Tao, J., Sun, Y. E., and Hsieh-Wilson, L. C. (2010) Quantification of O-glycosylation stoichiometry and dynamics using resolvable mass tags. *Nat. Chem. Biol.* *6*, 645–651.

(25) Leney, A. C., and Heck, A. J. R. (2017) Native MS: What's in the name? *J. Am. Soc. Mass Spectrom.* *28* (1), 5–13.

(26) Rose, R. J., Damoc, E., Denisov, E., Makarov, A., and Heck, A. J. R. (2012) High-sensitivity Orbitrap mass analysis of intact macromolecular assemblies. *Nat. Methods* *9*, 1084–1086.

(27) Rosati, S., Rose, R. J., Thompson, N. J., van Duijn, E., Damoc, E., Denisov, E., Makarov, A., and Heck, A. J. R. (2012) Exploring an Orbitrap Analyzer for the Characterization of Intact Antibodies by Native Mass Spectrometry. *Angew. Chem., Int. Ed.* *51*, 12992–12996.

(28) van de Waterbeemd, M., Lössl, P., Gautier, V., Marino, F., Yamashita, M., Conti, E., Scholten, A., and Heck, A. J. R. (2014) Simultaneous assessment of kinetic, site-specific, and structural aspects of enzymatic protein phosphorylation. *Angew. Chem., Int. Ed.* *53*, 9660–9664.

(29) Pathak, S., Borodkin, V. S., Albarbarawi, O., Campbell, D. G., Ibrahim, A., and van Aalten, D. M. (2012) O-GlcNAcylation of TAB1 modulates TAK1-mediated cytokine release. *EMBO J.* *31*, 1394–1404.

- (30) Tarrant, M. K., Rho, H.-S., Xie, Z., Jiang, Y. L., Gross, C., Culhane, J. C., Yan, G., Qian, J., Ichikawa, Y., Matsuoka, T., Zachara, N., Etkorn, F. A., Hart, G. W., Jeong, J. S., Blackshaw, S., Zhu, H., and Cole, P. A. (2012) Regulation of CK2 by phosphorylation and O-GlcNAcylation revealed by semisyn-thesis. *Nat. Chem. Biol.* 8, 262–269.
- (31) Sakurai, H. (2012) Targeting of TAK1 in inflammatory disorders and cancer. *Trends Pharmacol. Sci.* 33, 522–530.
- (32) Meggio, F., and Pinna, L. A. (2003) One-thousand-and-one substrates of protein kinase CK2? *FASEB J.* 17, 349–368.
- (33) Niefind, K., Guerra, B., Ermakowa, I., and Issinger, O. G. (2001) Crystal structure of human protein kinase CK2: insights into basic properties of the CK2 holoenzyme. *EMBO J.* 20, 5320–5331.
- (34) Pathak, S., Alonso, J., Schimpl, M., Rafie, K., Blair, D. E., Borodkin, V. S., Schüttelkopf, A. W., Albarbarawi, O., and van Aalten, D. M. F. (2015) The active site of O-GlcNAc transferase imposes constraints on substrate sequence. *Nat. Struct. Mol. Biol.* 22, 744–750.
- (35) Lössl, P., Brunner, A. M., Liu, F., Leney, A. C., Yamashi-ta, M., Scheltema, R. A., and Heck, A. J. R. (2016) Decipher-ing the Interplay among Multisite Phosphorylation, Interac-tion Dynamics, and Conformational Transitions in a Tripar-tite Protein System. *ACS Cent. Sci.* 2, 445–455.
- (36) Nishikawa, I., Nakajima, Y., Ito, M., Fukuchi, S., Homma, K., and Nishikawa, K. (2010) Computational Prediction of O-linked Glycosylation Sites that Preferentially Map on Intrin-sically Disordered Regions of Extracellular Proteins. *Int. J. Mol. Sci.* 11, 4991–5008.
- (37) Fontana, A., de Laureto, P. P., Spolaore, B., Frare, E., Picotti, P., and Zamboni, M. (2004) Probing protein structure by limited proteolysis. *Acta Biochim. Polonica* 51, 299–321.
- (38) Schimpl, M., Zheng, X., Borodkin, V. S., Blair, D. E., Ferenbach, A. T., Schüttelkopf, A. W., Navratilova, I., Aristo-telous, T., Albarbarawi, O., Robinson, D. A., Macnaughtan, M. A., and van Aalten, D. M. F. (2012) O-GlcNAc transferase invokes nucleotide sugar pyrophosphate participation in catalysis. *Nat. Chem. Biol.* 8, 969–974.
- (39) Lolli, G., Ranchio, A., and Battistutta, R. (2014) Active form of the protein kinase CK2 $\alpha 2\beta 2$ holoenzyme is a strong complex with symmetric architecture. *ACS Chem. Biol.* 9, 366–371.
- (40) Myers, S. A., Daou, S., Affar, E. B., and Burlingame, A. (2013) Electron transfer dissociation (ETD): the mass spec-trometric breakthrough essential for O-GlcNAc protein site assignments-a study of the O-GlcNAcylated protein host cell factor C1. *Proteomics* 13, 982–991.
- (41) Wells, J. M., and McLuckey, S. A. (2005) Collision-induced dissociation (CID) of peptides and proteins. *Methods Enzymol.* 402, 148–185.
- (42) Hunter, T. (2007) The age of crosstalk: phosphorylation, ubiquitination, and beyond. *Mol. Cell* 28, 730–738.